



Cite this: *Chem. Commun.*, 2025, 61, 9940

Received 6th May 2025,  
Accepted 26th May 2025

DOI: 10.1039/d5cc02577j

rsc.li/chemcomm

## Cross-linking teichoic acids by click chemistry prevents bacterial cell growth†

Morgane Baudoin,<sup>a</sup> Anne Chouquet,<sup>b</sup> Célia Boyat,<sup>b</sup> Cédric Laguri,<sup>b</sup> André Zapun,<sup>b</sup> Basile Pérès,<sup>a</sup> Cecile Morlot,<sup>b</sup> Yung-Sing Wong<sup>b</sup> \*<sup>a</sup> and Claire Durmort<sup>b</sup> \*<sup>b</sup>

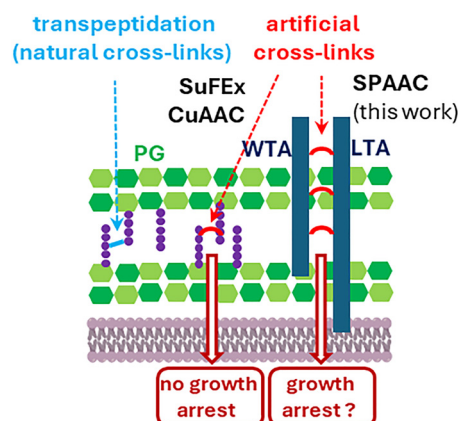
**This work identifies a novel antibacterial mechanism that targets the cell wall of the human pathogen *Streptococcus pneumoniae*. Unlike conventional cell-wall targeting antibiotics, which inhibit the natural cross-linking of peptidoglycan, we introduce artificial cross-links in the other main component of the Gram-positive cell wall, the teichoic acids, and show that it leads to impaired cell growth.**

Faced with the growing problem of antibiotic resistance, the discovery of new antibacterial targets remains a high priority.<sup>1</sup> The bacterial cell wall is a prime target that has already led to valuable antibiotics such as penicillin and vancomycin.<sup>2,3</sup> Its main component, peptidoglycan (PG, Fig. 1), is a biopolymer composed of repeating units of  $\beta$ -1,4-linked *N*-acetylglucosamine (GlcNAc) and *N*-acetylmuramic acid (MurNAc) (green in Fig. 1). MurNAc residues harbor peptide stems (purple in Fig. 1) that can cross-link to other PG strands, forming a mesh-like structure. During bacterial growth and division, PG synthesis and remodeling ensure cell morphogenesis, and resistance to cytoplasmic turgor pressure.

PG biosynthesis is targeted by several classes of antibiotics, leading to growth arrest and breaches in the PG mesh, ultimately causing cell lysis. In search of new antibacterial mechanisms, a key question is whether introducing unnatural cross-links into the cell wall can impair bacterial growth. Schultz *et al.* first achieved synthetic PG cross-linking in *Escherichia coli*<sup>4</sup> and *Bacillus subtilis*<sup>5</sup> by metabolically incorporating *D*-alanine analogues bearing a latent electrophilic sulfonyl fluoride group. Following SuFEx click chemistry,<sup>6</sup> these analogues could subsequently cross-link with a neighboring nucleophile (proximity-induced ligation). No significant effect on bacterial growth was observed, except in *B. subtilis*  $\Delta$ *dacA*, a strain lacking the *D*-Ala-*D*-Ala carboxypeptidase PBP5. In this mutant, enhanced persistence of the *D*-alanine analogue led to high levels of unnatural cross-linking, resulting in slower growth

and cell shape defects (elongated and curly cells). Later, Siegrist *et al.* incorporated *D*-alanine derivatives bearing azido and alkyne groups into PG, with cross-linking subsequently induced by CuAAC.<sup>7</sup> Again, no impact on growth was noticed, and contrary to the desired effect, a protection against broad-spectrum  $\beta$ -lactams was reported.

The Gram-positive bacterial cell wall contains another biopolymer, teichoic acids (TAs, deep blue in Fig. 1), made of repeating phosphate, saccharide, *N*-acetylgalactosamine and alditol groups. There are two types: wall teichoic acids (WTAs), covalently bound to PG, and lipoteichoic acids (LTAs), anchored in the cytoplasmic membrane. TAs are involved in numerous cellular processes that include cell elongation and division, and maintenance of the Gram-positive periplasmic space, which helps resist turgor pressure.<sup>8,9</sup> In this context, we investigated whether TA cross-linking could impair bacterial growth. We exploited the fact that *S. pneumoniae* TAs are decorated with phosphocholines, which can be selectively replaced by clickable choline analogues.<sup>10–12</sup> Here, we evaluated the incorporation efficiency of various choline



Gram-positive bacteria cell wall

**Fig. 1** Structure of the cell wall of Gram-positive bacteria and illustration of the artificial cross-linking mechanisms described in previous publications with peptidoglycan (PG)<sup>4–6</sup> and in this work with teichoic acids (TAs).

<sup>a</sup> Univ. Grenoble Alpes, CNRS, DPM, 38000 Grenoble, France.

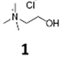
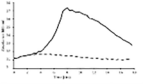
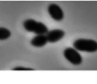
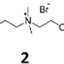
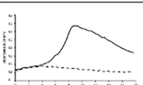
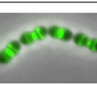
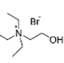
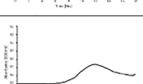
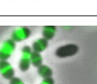
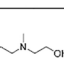
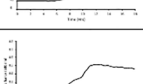
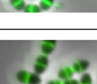
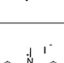
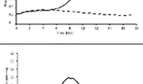
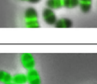
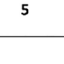
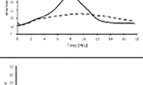
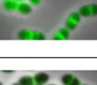
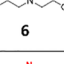
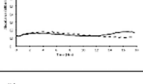
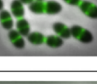
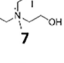
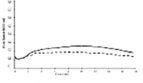
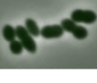
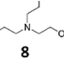
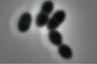
E-mail: yung-sing.wong@univ-grenoble-alpes.fr

<sup>b</sup> Univ. Grenoble Alpes, CNRS, CEA, IBS, 38000 Grenoble, France.

E-mail: claire.durmort@ibs.fr

† Electronic supplementary information (ESI) available. See DOI: <https://doi.org/10.1039/d5cc02577j>



Compound	Growth curve in the presence of compounds	Pattern of labelling	Intensity of labelling	Competition with ClCho (%)
 <b>1</b>			ND	100
 <b>2</b>			100	49
 <b>3</b>			163 ± 24	12
 <b>4</b>			120 ± 24	12
 <b>5</b>			174 ± 44	53
 <b>6</b>			62 ± 26	9
 <b>7</b>			ND	ND
 <b>8</b>			ND	ND
 <b>9</b>	ND		ND	ND

**Fig. 2** Incorporation of various azido-cholines in the capsule-free *S. pneumoniae* D39  $\Delta$ cps strain, followed by fluorescent labelling. Growth curves in the presence of compounds **1** to **9** (full line) or without choline (dashed line) were obtained by measuring the optical density (600 nm) of the cell cultures. Merged images between phase contrast and AF488 channels show the localization patterns of labelled TAs. Scale bars, 1  $\mu$ m. The relative fluorescence intensity of labelled D39  $\Delta$ cps cells analyzed by flow cytometry is given as a percentage of the fluorescence intensity measured for compound **2** ( $n = 3$ ). The relative fluorescence intensity of D39  $\Delta$ cps cells labelled with compounds **1** to **9** in competition with choline chloride **1** (ClCho), analyzed by flow cytometry, is expressed as a percentage of the value obtained without choline chloride **1** ( $n = 2$ ). ND: not detectable.

analogues into *S. pneumoniae* TAs, and explored the cross-linking of one analogue with an additional agent to artificially interconnect TAs and potentially hinder bacterial growth.

We first aimed to determine if choline metabolization into the TA can tolerate structural and functional variations of the clickable motifs. The SPAAC reaction was chosen because it involves the small azido group. The different types of “choline-like” azido compounds (Fig. 2) were inspired by the work of Tomasz, who reported that in the absence of choline in the growth medium, *S. pneumoniae* is able to incorporate ethanol amine instead, demonstrating that the presence of a tetra-alkyl ammonium function is not mandatory.<sup>13,14</sup> Interestingly, Badger also showed that *S. pneumoniae* can grow in the presence of tri-alkylated ethanol amine (tertiary amines), but they did not demonstrate that tri-alkylated ethanol amine is actually incorporated into

the TA.<sup>15</sup> In addition to the conventional azido compound **2**,<sup>11</sup> its di-ethylated analogue **3** and the corresponding tertiary amine **4** were made.

Two analogues with a longer alkyl chain containing an azido group, the ammonium analogue **5** and the tertiary amine **6**, were also synthesized, as well as the quaternary ammonium analogue **7** and tertiary amine **8** bearing two ethanol groups. Finally, a bulky group, inspired by the fluorogenic azido-coumarin<sup>16</sup> used by Siegrist *et al.*,<sup>7</sup> was grafted onto the choline unit to generate compound **9**.

These molecules were evaluated based on three criteria: their impact on bacterial growth, their labelling efficiency during a 10 minute pulse-labelling period (Fig. S1, see ESI<sup>†</sup>), and their competitiveness compared to the incorporation of native choline (Fig. 2). Incorporation of the modified choline into TA was carried out at the same time as fluorescent labelling with DBCO-AF488 in C-medium, as reported previously.<sup>12</sup> Fluorescence intensities were measured by flow cytometry, and the mean value obtained with compound **2** was defined as the reference. The incorporation of choline **2** into TA was also shown by NMR analysis of the LTA extract (Fig. 3 and Fig. S3, see ESI<sup>†</sup>). For pulse labelling, the quaternary ammonium compounds **2**, **3** and **5** were globally effective, while the di-ethanol analogue **7** was inefficient. For tertiary amine analogues **4** and **6**, fluorescence microscopy showed for the first time their incorporation into TA, albeit with less efficiency for compound **6** ( $62 \pm 26\%$ ,  $p < 0.05$ ), which harbors the longest alkyl chain. The azido-coumarin choline compound **9** was used with DIBO **10** to trigger a fluorogenic labelling,<sup>7,16</sup> but no fluorescent signal was observed, indicating that the choline derivative was not incorporated by the bacteria, probably due to its bulkiness. Analysis of the bacterial growth rate showed that, compared to native choline, compound **2** is the least harmful of all the choline derivatives (Fig. S2, see ESI<sup>†</sup>). Taken together, these observations show that the metabolic incorporation of modified choline and bacterial cell growth tolerate moderate hindrance and modification. Incorporation into TA seems more permissive to choline modifications than cell growth, as illustrated by the data obtained with the quaternary ammonium compounds **3** and **5**, and the tertiary amine compounds **4** and **6**, which allow TA labelling but impair cell growth (Fig. 2).

Following TA labelling with compound **2**, the next step was to cross-link these polymers using the external agent **11**, which

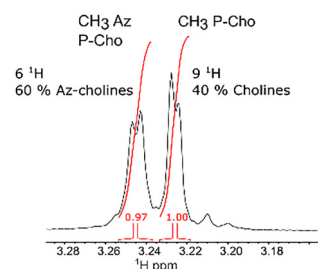


**Fig. 3** Portion of the 1D  $^1\text{H}$  spectrum of LTAs labelled with azido-choline **2**, shown in Fig. S3 (see ESI<sup>†</sup>). The peaks corresponding to the methyl groups of choline and azido-choline were integrated, revealing a 60% content of azido-choline in the LTA sample.



has two DBCO groups on a polyethylene glycol chain (Fig. 4 and Fig. S4, see ESI†). To compare the effect of TA cross-linking with that of artificial PG cross-linking, we used azido-D-alanine (azido-DADA) **12**,<sup>17–19</sup> which places an azido group at position 4 of the pentapeptide stem in the PG. The concentrations were set at 250  $\mu$ M and 2 mM for optimal incorporation of analogues **2** and **12**, respectively. Bacteria were first treated for 10 min (pulse 1, Fig. S4, ESI†) with either native choline **1**, azido-choline **2**, azido-DADA **12**, or both compounds **2** and **12**, in chemically defined C-medium.<sup>20</sup> After centrifugation to remove excess compounds, cells were resuspended in brain-heart infusion (BHI) medium with or without linker **11** (100  $\mu$ M), and incubated for 10 min (pulse 2). Cultures were then diluted 30-fold in BHI and grown overnight in 24-well plates. When TAs were labelled with azido-choline **2**, a 10 min incubation with 100  $\mu$ M linker **11** significantly inhibited growth ( $57 \pm 9\%$  relative to the control without linker **11**). To allow the SPAAC reaction to continue after the dilution into the growth medium, linker **11** was further added as a supplement at 10  $\mu$ M, reducing the growth rate ratio to  $25 \pm 12\%$ , relative to the control condition. At 10  $\mu$ M, linker **11** showed no toxicity of its own. In the presence of 50  $\mu$ M linker **11**, the relative growth rate was reduced to  $7 \pm 2\%$ . However, this was possibly due to a slight intrinsic toxicity of **11** at high concentration, as found in the control condition with choline **1** and 50  $\mu$ M linker **11** ( $64 \pm 6\%$ ). In contrast, the use of azido-DADA **12** and linker **11** did not significantly impact growth, suggesting that synthetic PG cross-links do not strongly impair cell growth, as previously reported for *E. coli* and *B. subtilis*.<sup>4,5</sup> The reduced growth seen with azido-DADA **12** and 50  $\mu$ M linker **11** ( $56 \pm 1\%$  relative to the control condition) was quite similar to that of choline **1** with 50  $\mu$ M linker **11** ( $64 \pm 6\%$ ), supporting a toxic effect of linker **11** at this concentration. It is noteworthy to observe that the joint addition of azido-choline **2** and azido-DADA

**12** reproduced the same growth defect as the single addition of azido-choline **2**. Therefore, there is no additional effect due to possible cross-linking between TA and PG. In a bacterium lacking choline-decorated TA like *B. subtilis*, incubation with azido-choline **2** and linker **11** had no impact on growth (Fig. S5, see ESI†). Similarly, *E. coli*, which lacks TA in its cell wall, was unaffected by the compounds.

To assess the impact of cross-linking on cell wall synthesis, *S. pneumoniae* cells treated with azido-choline **2** and linker **11** were incubated with a DBCO-linked fluorophore for 10 min (chase period, Fig. 5 and Fig. S6, see ESI†). Remaining free azido functions on TA were conjugated with the DBCO-fluorophore by SPAAC reaction. The distance between fluorescent bands reflects wall synthesis at the midcell following TA cross-linking. Demograph analysis (Fig. 5) revealed that linker **11** inhibited wall expansion, with a significant decrease of the mean distance between labelled bands (0.77 nm to 0.45 nm in the absence and presence of linker **11**, respectively;  $p < 0.01$ ). With longer chase periods (20, 40 and 60 min, Fig. 6), minimal change in the fluorescent banding patterns was observed, with most cells retaining midcell labelling. In contrast, cells not treated with linker **11** showed normal division, progressively diluting the initial fluorescence signal over time.

To confirm TA cross-linking, we applied our recently developed gel electrophoresis and fluorescence imaging method (Fig. 7 and Fig. S7, see ESI†).<sup>9</sup> Cells labelled with azido-choline **2**, with or without linker **11**, were treated with PG hydrolases to digest the cell wall. Remaining free azido or DBCO groups were then reacted with complementary fluorophore-linked probes. Samples were analyzed by tris-tricine SDS-PAGE, and labelled species were visualized under UV. LTAs appeared as a ladder due to their lipidic nature and SDS interaction, whereas WTAs migrated as an upper smear bound to PG fragments. In the presence of linker **11**, the LTAs shifted upward and became unresolved, with additional high-

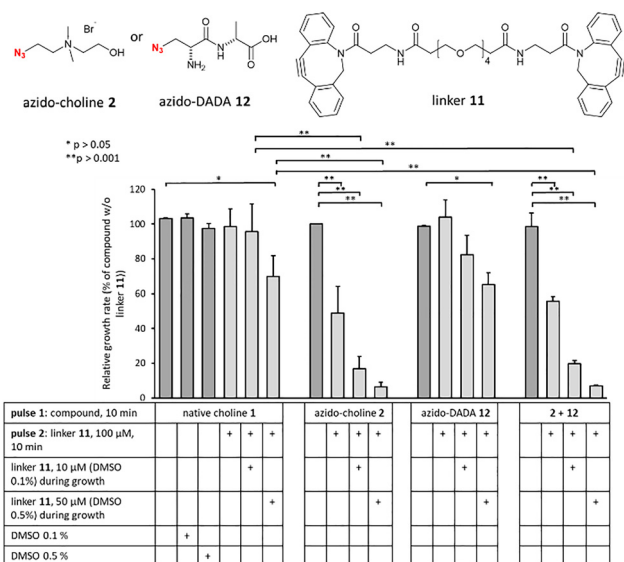


Fig. 4 Growth arrest induced by TA crosslinking. Growth rate ratio in the various culture conditions is reported relative to that in the presence of choline or DADA derivative and in the absence of linker **11** (taken as 100%). Growth was monitored in a microplate reader by measuring the absorbance at 600 nm ( $n = 4$ ).

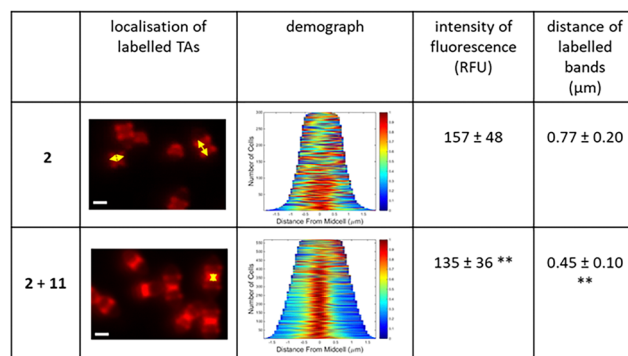
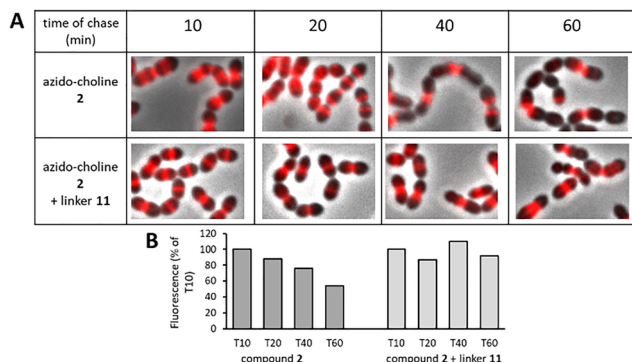


Fig. 5 Effect of TA cross-linking on *S. pneumoniae* growth. D39  $\Delta$ cps cells were incubated in C-medium without choline containing 250  $\mu$ M azido-choline **2**. Cells were then grown in BHI without or with 100  $\mu$ M of linker **11** before labelling with DBCO-AF647. Cells were analysed by fluorescent microscopy and flow cytometry. Fluorescence microscopy images show the localization of labelled TAs (yellow narrow). Scale bars, 1  $\mu$ m. The mean of fluorescence intensity ( $\pm$ SD) was calculated from cytometry data. The demographs show the fluorescence profiles of labelled D39  $\Delta$ cps cells, ordered by ascending length. The mean of the distance separating the labelled bands ( $\pm$ SD,  $n = 200$ ) reflects the growth of the cell population (\*\* $p < 0.001$ , unpaired test).







**Fig. 6** Evolution of the localization of labelled TAs during cell growth. After TA labelling with 250  $\mu$ M azido-choline **2** and further incubation without or with 100  $\mu$ M linker **11**, cell culture was performed for 60 min in BHI medium. At each time point, cells were analysed by fluorescence microscopy and flow cytometry. (A) Merged images of the phase contrast and AF647 channels. Scale bars, 1  $\mu$ m. (B) The relative fluorescence of the population, calculated from the flow cytometry data, is presented as a percentage of the value measured at T10.

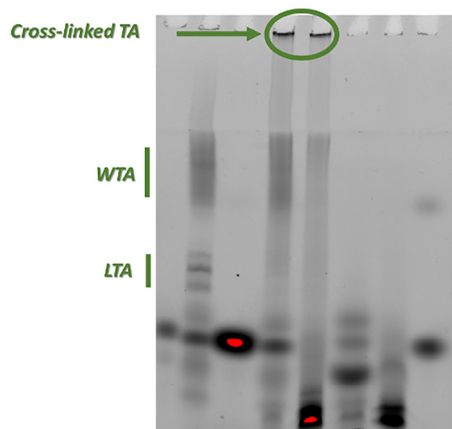


**Fig. 7** Gel electrophoresis analysis of TA. After metabolic labeling with **2**, and cross-linking with **11**, cells were lysed and free remaining clickable groups were fluorescently labelled. Labelled species were separated by polyacrylamide gel electrophoresis and observed by UV-trans-illumination. The positions of lipoteichoic acids (LTAs), wall teichoic acids (WTAs) and cross-linked TAs are indicated.

molecular-weight species retained in the wells. The appearance of these large, low electrophoretic mobility species indicates successful TA cross-linking *via* SPAAC between azido-choline **2** and linker **11**.

In conclusion, we have demonstrated that, unlike artificial PG cross-linking, TA cross-linking can inhibit the growth of *S. pneumoniae*. This growth inhibition may be explained by a much higher grafting yield of azido functions into TAs compared to PG, or by the fact that TAs are not cross-linked by nature (unlike PG). Whereas conventional cell-wall targeting antibiotics inhibit the natural cross-linking of the bacterial wall, our mechanism operates in the opposite way, by

artificially inducing cross-linking where none normally occurs. This entirely new mode of action constitutes a novel and promising therapeutic target, particularly relevant in the pre-occupying context of antimicrobial resistance.

We acknowledge the financial support for this work from Agence Nationale de la Recherche (ANR-19-CE07-0035 and ANR-23-CE11-0029). We thank R.-L. Revel-Goyet, O. Glushonkov and J.-P. Kleman (IBS, Grenoble) for support and access to the M4D cell imaging platform. This work used the platforms of the Grenoble Instruct-ERIC center (ISBG; UAR 3518 CNRS-CEA-UGA-EMBL) within the Grenoble Partnership for Structural Biology (PSB), supported by FRISBI (ANR-10-INBS-0005-02) and Labex ARCANE and Labex GRAL, financed within the University Grenoble Alpes graduate school (Ecoles Universitaires de Recherche) CBH-EUR-GS (ANR-17-EURE-0003). IBS acknowledges integration into the Interdisciplinary Research Institute of Grenoble (IRIG, CEA). The authors acknowledge support from Institut de Chimie Moléculaire de Grenoble (ICMG, UAR 2607) for analysis facilities.

## Data availability

Data presented in this work are available within the article and/or its ESI,<sup>†</sup> and upon request to the authors.

## Conflicts of interest

There are no conflicts to declare.

## Notes and references

- 1 L. Chen, S. Kumar and H. Wu, *Arch. Microbiol.*, 2023, **205**, 356.
- 2 M. F. Chellat, L. Raguz and R. Riedl, *Angew. Chem., Int. Ed.*, 2016, **55**, 6600.
- 3 H. Cho, *J. Microbiol.*, 2023, **61**, 359.
- 4 D. A. Dik, N. Zhang, J. S. Chen, B. Webb and P. G. Schultz, *J. Am. Chem. Soc.*, 2020, **142**, 10910.
- 5 D. A. Dik, N. Zhang, E. J. Sturgell, B. B. Sanchez, J. S. Chen, B. Webb, K. G. Vanderpool and P. G. Schultz, *Proc. Natl. Acad. Sci. U. S. A.*, 2021, **118**, e2100137118.
- 6 J. Dong, L. Krasnova, M. G. Finn and K. B. Sharpless, *Angew. Chem., Int. Ed.*, 2014, **53**, 9430.
- 7 S. L. Rivera, A. Espallat, A. K. Aditham, P. Shieh, C. Muriel-Mundo, J. Kim, F. Cava and M. S. Siegrist, *Cell Chem. Biol.*, 2021, **28**, 213.
- 8 H. P. Erickson, *Front. Microbiol.*, 2021, **12**, 664704.
- 9 M. Nguyen, E. Bauda, C. Boyat, C. Laguri, C. Freton, A. Chouquet, B. Gallet, M. Baudoin, Y.-S. Wong, C. Grangeasse, C. Moriscot, C. Durmort, A. Zapun and C. Morlot, *eLife*, 2025, **14**, RP105132.
- 10 A. Tomasz, *Science*, 1967, **157**, 694.
- 11 A.-M. Di Guilmi, J. Bonnet, S. Peibert, C. Durmort, B. Gallet, T. Vernet, N. Gisch and Y.-S. Wong, *Chem. Commun.*, 2017, **53**, 10572.
- 12 J. Bonnet, Y.-S. Wong, T. Vernet, A.-M. Di Guilmi, A. Zapun and C. Durmort, *ACS Chem. Biol.*, 2018, **13**, 2010.
- 13 A. Tomasz, *Proc. Natl. Acad. Sci. U. S. A.*, 1968, (59), 86–93.
- 14 T. Briesse and R. Hakenbeck, *Eur. J. Biochem.*, 1985, **146**, 417.
- 15 E. Badger, *J. Biol. Chem.*, 1944, **153**, 183.
- 16 K. Sivakumar, F. Xie, B. M. Cash, S. Long, H. N. Barnhill and Q. Wang, *Org. Lett.*, 2004, **6**, 4603.
- 17 G. W. Liechti, E. Kuru, E. Hall, A. Kalinda, Y. V. Brun, M. VanNieuwenhze and A. T. Maurelli, *Nature*, 2014, **506**, 507.
- 18 J. Trouve, A. Zapun, C. Arthaud, C. Durmort, A.-M. Di Guilmi, B. Söderström, A. Pelletier, C. Grangeasse, D. Bourgeois, Y.-S. Wong and C. Morlot, *Curr. Biol.*, 2021, **31**, 2844.
- 19 E. Kuru, A. Radkov, X. Meng, A. Egan, L. Alvarez, A. Dowson, G. Boher, E. Breukink, D. I. Roper, F. Cava, W. Vollmer, Y. Brun and M. VanNieuwenhze, *ACS Chem. Biol.*, 2019, **14**, 2745.
- 20 S. Lacks and R. D. Hotchkiss, *Biochim. Biophys. Acta*, 1960, **39**, 508.

